



**HAL**  
open science

## Chemical Delivery System of MIBG to the Central Nervous System: Synthesis, <sup>11</sup>C-Radiosynthesis, and in Vivo Evaluation

Fabienne Gourand, Delphine Patin, Axelle Henry, Meziiane Ibazizeñe, Martine Dhilly, Fabien Fillesoye, Olivier Tirel, Mihaela-Liliana Tintas, Cyril Papamicael, Vincent Levacher, et al.

### ► To cite this version:

Fabienne Gourand, Delphine Patin, Axelle Henry, Meziiane Ibazizeñe, Martine Dhilly, et al.. Chemical Delivery System of MIBG to the Central Nervous System: Synthesis, <sup>11</sup>C-Radiosynthesis, and in Vivo Evaluation. ACS Medicinal Chemistry Letters, 2019, 10 (3), pp.352-357. 10.1021/acsmchemlett.8b00642 . hal-03020265

**HAL Id: hal-03020265**

**<https://hal.science/hal-03020265v1>**

Submitted on 23 Nov 2020

**HAL** is a multi-disciplinary open access archive for the deposit and dissemination of scientific research documents, whether they are published or not. The documents may come from teaching and research institutions in France or abroad, or from public or private research centers.

L'archive ouverte pluridisciplinaire **HAL**, est destinée au dépôt et à la diffusion de documents scientifiques de niveau recherche, publiés ou non, émanant des établissements d'enseignement et de recherche français ou étrangers, des laboratoires publics ou privés.

# 1 Chemical Delivery System of MIBG to the Central Nervous System: 2 Synthesis, <sup>11</sup>C-Radiosynthesis, and *in Vivo* Evaluation

3 Fabienne Gourand,<sup>\*,‡</sup> Delphine Patin,<sup>‡</sup> Axelle Henry,<sup>†</sup> Méziane Ibazizène,<sup>‡</sup> Martine Dhilly,<sup>‡</sup>  
4 Fabien Fillesoye,<sup>‡</sup> Olivier Tirel,<sup>‡</sup> Mihaela-Liliana Tintas,<sup>‡</sup> Cyril Papamicaël,<sup>†</sup> Vincent Levacher,<sup>\*,†</sup>  
5 and Louisa Barré<sup>‡</sup>

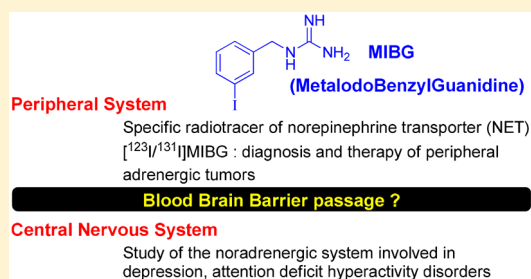
6 <sup>‡</sup>Normandie Univ, UNICAEN, CEA, CNRS, UMR 6030 ISTCT/LDM-TEP group, Bd Henri Becquerel, BP 5229, 14074 Cedex  
7 Caen, France

8 <sup>†</sup>Normandie Univ, COBRA, UMR 6014 et FR 3038; Univ Rouen; INSA Rouen; CNRS, IRCOF, 1 rue Tesnière, 76821 Mont Saint  
9 Aignan Cedex, France

## 10 **S** Supporting Information

11 **ABSTRACT:** The norepinephrine transporter (NET) plays an impor-  
12 tant role in neurotransmission and is involved in a multitude of  
13 psychiatric and neurodegenerative diseases. [<sup>123</sup>I/<sup>131</sup>I]meta-iodobenzyl-  
14 guanidine (MIBG) is a widely used radiotracer in the diagnosis and  
15 follow-up of peripheral neuroendocrine tumors overexpressing the  
16 norepinephrine transporter. MIBG does not cross the blood–brain  
17 barrier (BBB), and we have demonstrated the “proof-of-concept” that 1,4-  
18 dihydroquinoline/quinolinium salt as chemical delivery system (CDS) is  
19 a promising tool to deliver MIBG to the brain. To improve BBB passage,  
20 various substituents on the 1,4-dihydroquinoline moiety and a linker  
21 between CDS and MIBG were added. A series of CDS-MIBGs **1a–d** was synthesized, labeled with carbon-11, and evaluated *in*  
22 *in vivo* into rats. The *in vivo* results demonstrated that, although adding substituents on CDS in **1a–c** is of no benefit for brain  
23 delivery of MIBG, the presence of a linker in CDS-MIBG **1d** greatly improved both brain penetration and the release rate of  
24 MIBG in the central nervous system.

25 **KEYWORDS:** Central nervous system, norepinephrine transporter, MIBG, radiosynthesis, redox chemical delivery system,  
26 1,4-dihydroquinolines carriers



27 **T**he *in vivo* expression of norepinephrine transporter  
28 (NET) is mostly established in the central and peripheral  
29 sympathetic nervous system. Several different radiotracers for  
30 clinical imaging of NET expression were developed.

31 Among them, meta-iodobenzylguanidine (MIBG) is struc-  
32 turally similar to the neurotransmitter norepinephrine, and  
33 [<sup>123</sup>I]MIBG single photon emission computed tomography  
34 (SPECT) imaging studies are the most accurate method for  
35 detection of catecholamine-secreting tumors including neuro-  
36 endocrine tumors such as pheochromocytoma and neuro-  
37 blastoma.<sup>1–3</sup>

38 Moreover, MIBG was also radiolabeled with iodine-131 for  
39 radiotherapy to treat neuroendocrine tumors. Positron  
40 emission tomography (PET) is more accurate and has the  
41 potential to be more sensitive and to provide better image  
42 resolution. In this context, efforts to develop MIBG analogs  
43 labeled with a positron emitter remain of great interest, and  
44 several <sup>18</sup>F-labeled benzylguanidine analogs have already been  
45 developed for PET imaging of NET expression. Recently, the  
46 radiotracer meta-[<sup>18</sup>F]Fluorobenzylguanidine ([<sup>18</sup>F]MFBG)  
47 has shown to be a very promising PET candidate leading to  
48 successful clinical investigations.<sup>4–7</sup> Dysregulation of NET is  
49 implicated in various neuropsychiatric disorders such as

depression, anxiety, attention deficit hyperactivity disorders  
50 (ADHD), Parkinson’s disease, Alzheimer’s disease, and  
51 epilepsy. As the NET plays an important role in the central  
52 nervous system (CNS), the use of MIBG or MIBG analogs in  
53 brain imaging needs to be explored. However, MIBG is unable  
54 to cross the blood–brain-barrier (BBB). Guilloteau et al. have  
55 compared the uptake and release of radioiodinated meta-  
56 iodobenzylguanidine ([<sup>125</sup>I]MIBG) and tritiated norepineph-  
57 rine ([<sup>3</sup>H]NE) in different regions of the rat brain. The authors  
58 found comparable regional distribution of [<sup>3</sup>H]NE and  
59 [<sup>125</sup>I]MIBG uptake in the rat brain.<sup>8</sup> A chemical delivery  
60 system (CDS) designed for MIBG able to cross the BBB would  
61 provide a potential imaging marker to visualize the NET in the  
62 brain (Figure 1). In the literature, Bodor et al. have developed  
63 an interesting CDS based on a lipophilic 1,4-dihydropyridine  
64 able to cross the lipophilic BBB.<sup>9,10</sup> Then, the 1,4-  
65 dihydropyridine system is oxidized into the CNS to a  
66 hydrophilic pyridinium species, which cannot cross back the  
67 BBB (named as “the locked in effect”). A subsequent  
68

**Received:** December 18, 2018

**Accepted:** February 15, 2019

**Published:** February 15, 2019

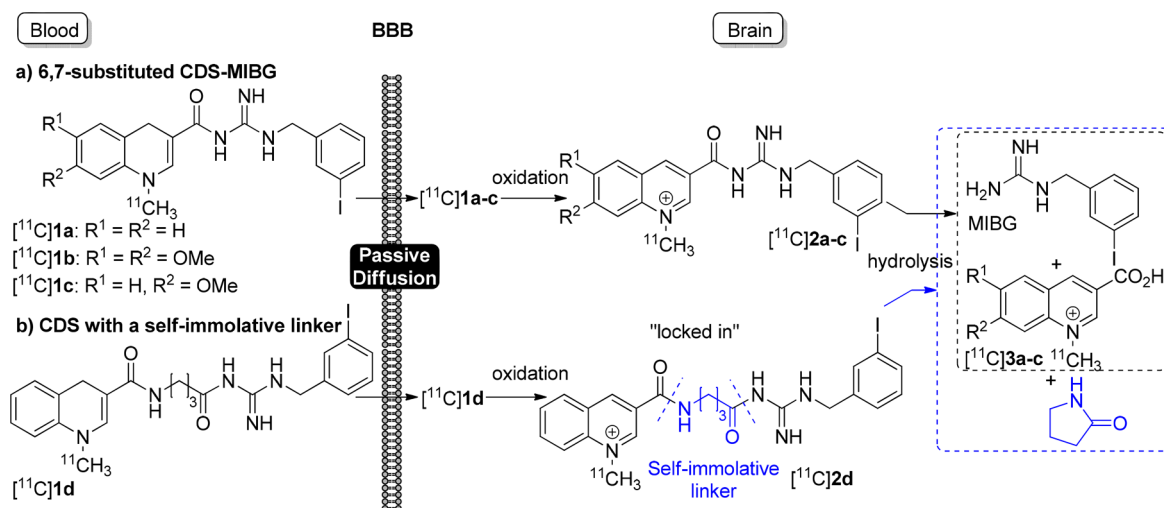
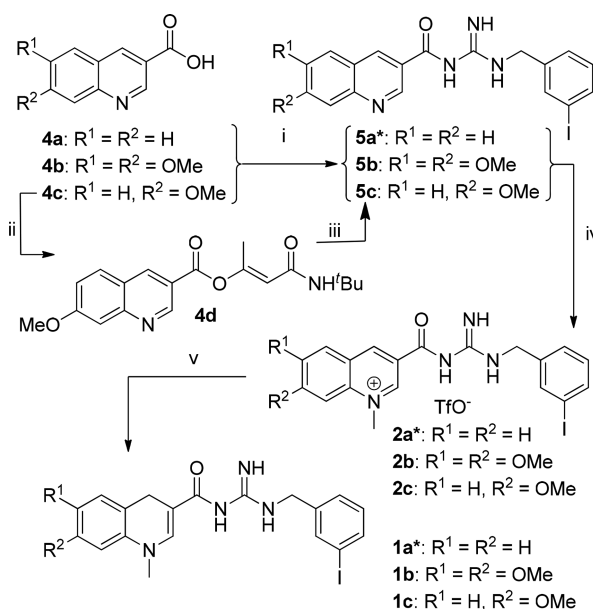


**Figure 1.** Development of a  $^{11}\text{C}$ -chemical delivery system of MIBG into the CNS.

69 hydrolysis releases the active compound, which can then act  
 70 directly on the target into the CNS. By using this approach,  
 71 Bodor et al. have targeted many drugs to the CNS.<sup>11–14</sup> Later,  
 72 Levacher et al. have solved many drawbacks related to this  
 73 CDS by means of 1,4-dihydroquinolines instead of 1,4-  
 74 dihydropyridines. However, although mainly drugs were  
 75 successfully targeted using this strategy, very few reports deal  
 76 with the use of this CDS to target radiotracers into the brain. A  
 77 survey of the literature indicated that, aside from our previous  
 78 work on MIBG,<sup>15,16</sup> only a single research article<sup>17</sup> explored  
 79 the potential of this appealing CDS approach to deliver a  
 80 radiolabeled agent into the CNS. As far as our preliminary  
 81 research work on MIBG is concerned, our initial work focused  
 82 on the radiolabeling with carbon-11 of the CDS in order to  
 83 validate the concept described previously. The results of the *in*  
 84 *vivo* studies were highly encouraging, supporting our working  
 85 hypothesis that the dihydroquinoline system may possibly be a  
 86 promising CDS to target MIBG to brain tissues. Indeed, after  
 87 *in vivo* injection into rats of  $[^{11}\text{C}]$ CDS-MIBG ( $[^{11}\text{C}]1\text{a}$ ), the  
 88 passage of  $[^{11}\text{C}]1\text{a}$  through the BBB has been demonstrated as  
 89 well as the presence of MIBG in the brain. However, this  
 90 chemical delivery system has some limitations: (1) a moderate  
 91 brain penetration has been measured, and (2) the oxidation  
 92 kinetics of  $[^{11}\text{C}]1\text{a}$  was quite slow since more than 50% was  
 93 still present in rat brain at 45 min post injection. For these  
 94 reasons, this CDS still needed to be optimized before being  
 95 applied to radioiodinated MIBG. This Letter will focus on the  
 96 preparation and *in vivo* evaluation of new 1,4-dihydroquino-  
 97 line-MIBG systems  $[^{11}\text{C}]1\text{b,c}$  bearing methoxy groups to tune  
 98 the redox potential of the CDS. The preparation and *in vivo*  
 99 evaluation of a 1,4-dihydroquinoline  $[^{11}\text{C}]1\text{d}$  having a self-  
 100 immolative linker between the CDS and MIBG will be also  
 101 reported (Figure 1).

102 To perform the radiosynthesis and *in vivo* study of our  
 103 systems, it was first necessary to synthesize the precursors for  
 104 radiolabeling and references that will be used to identify  
 105 compounds in radio-HPLC. We have previously described the  
 106 synthesis of the targeting system **1a** starting from quinoline **4a**  
 107 (Scheme 1).<sup>15</sup> We decided to adopt the same approach to  
 108 prepare **1b,c**. Thus, a coupling reaction from quinolines  
 109 **4b,c**<sup>18,19</sup> and MIBG using CDI led to the corresponding  
 110 quinolines **5b,c** in moderate yields (36% and 30%,  
 111 respectively). Alternatively, quinoline **5c** could be prepared

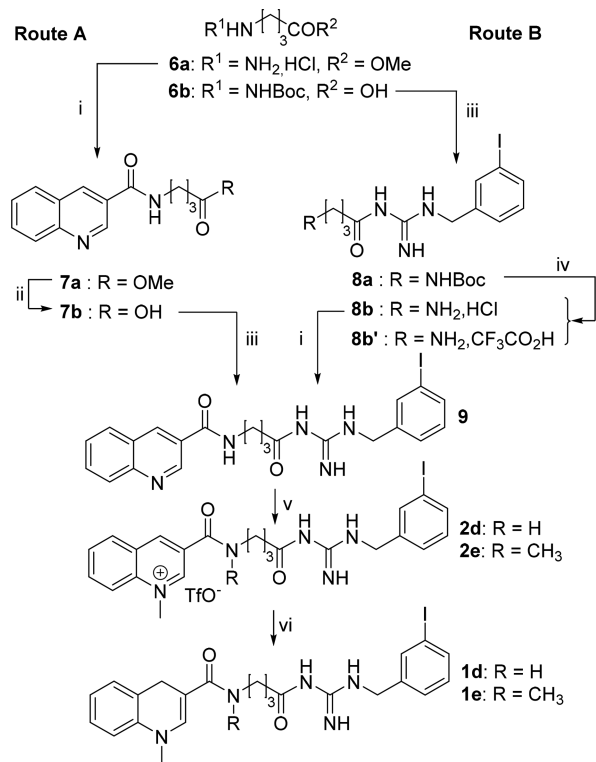
### Scheme 1. Synthesis of the Redox CDS-MIBG **1a–c**<sup>a</sup>



<sup>a</sup>Reagents and conditions: (i) CDI, DMF, 20 °C, 1 h then MIBG, 20 °C, 1 h for **5a\*** (60%) and **5b** (36%) and **5c** (30%); (ii) NBI,  $\text{NET}_3$ , DMF, 20 °C, 12 h (74%); (iii) MIBG, DMF, 140 °C, 7 h (76%); (iv)  $\text{CH}_3\text{OTf}$ ,  $\text{CH}_2\text{Cl}_2$ , 20 °C, 2 h for **2a\*** (50%), 3 h for **2b** (60%) and **2c** (81%); (v) BNAH,  $\text{CH}_2\text{Cl}_2$ , 20 °C, 12 h for **1a\*** (95%), **1b** (32%), **1c** (70%). **1a\***, **2a\*** and **5a\*** results are from ref 15.

by reacting MIBG with the activated enol ester<sup>20</sup> **4d** (76%),  
 the latter having been obtained by reacting **4c** with NBI (74%).  
 Then, quinolines **5b,c** were easily transformed into their  
 corresponding quinolinium salts **2b,c** (60% and 81%,  
 respectively) in the presence of methyl triflate. Finally, the  
 desired CDS-MIBG **1b,c** were successfully obtained after  
 regioselective reduction of quinolinium salts **2b,c** by means of  
 BNAH (32% and 70%, respectively).

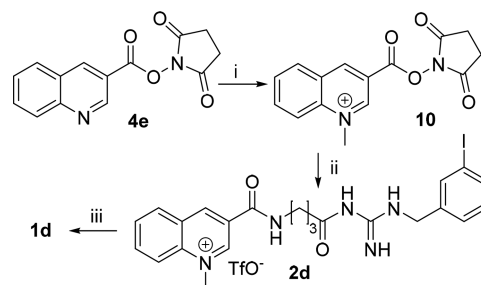
We next turned our attention to the synthesis of a CDS  
 having a  $\gamma$ -aminobutyric acid (GABA) self-immolative linker  
 group.<sup>21–23</sup> We envisaged the synthesis of quinoline **9** from  
 GABA derivative **6a** (Scheme 2, route A). So, neutralization of  
 hydrochloride amine salt **6a** and subsequent coupling reaction  
 with carboxylic acid **4a** using BOP reagent led to quinoline **7a**

Scheme 2. Initial Routes To Synthesize the Targeting System 1d<sup>a</sup>

<sup>a</sup>Reagents and conditions: (i) NaOH then **4a**, BOP,  $NEt_3$ , DMF, 20 °C, 12 h (79% for **7a**, 25% for **9**); (ii) LiOH, THF, MeOH,  $H_2O$ , 20 °C, 3 h (96%); (iii) BOP, MIBG,  $NEt_3$ , DMF, 20 °C, 12 h (25% for **8a**, 4% for **9**); (iv)  $CH_3COCl$ , MeOH, 20 °C, 1 h for **8b** (95%) or TFA,  $CH_2Cl_2$ , -5 °C, 1 h for **8b'** (98%); (v)  $CH_3OTf$ ,  $CH_2Cl_2$ , 20 °C, 12 h (44% for **2d** and 23% for **2e** determined by  $^1H$  NMR); (vi) BNAH,  $CH_2Cl_2$ , 20 °C, 12 h.

(79% yield). The methyl ester functional group was hydrolyzed by LiOH to give carboxylic acid **7b** (96% yield). The latter was subsequently involved in a coupling reaction with MIBG using BOP to give **9** in a very low yield (4% yield). We also investigated other activation strategies of carboxylic acid **7b** by means of CDI,  $ClCOOEt$ ,  $(COCl)$ , NBI, or NHS/DCC. Unfortunately, we failed to obtain **9** by using these reagents. Alternatively, *N*-protected GABA **6b** and MIBG were reacted in the presence of BOP reagent to furnish the coupling product **8a** in 25% yield (Scheme 2, route B). Then, *N*-Boc deprotection was carried out by using either acetyl chloride/MeOH or TFA to lead, respectively, to the desired ammonium salts **8b** and **8b'** (95% and 98% yields). One may note that 20 equiv of acetyl chloride/MeOH or TFA were required during the course of the *N*-Boc deprotection to prevent from the formation of the undesired  $\gamma$ -lactam ring resulting from the cyclization reaction of the self-immolative linker. Thereafter, ammonium **8b** was neutralized back to pH 7 with sodium hydroxide before being converted into the desired amide **9** in 25% yield by means of a coupling reaction between **4a** and BOP reagent. The quaternization reaction of **9** with methyl triflate afforded a mixture of **2d,e** (44% and 23%, respectively, estimated by  $^1H$  NMR). We then proceeded to a classical reduction of the mixture of quinolinium salts **2d,e** with BNAH. However, LC/MS analysis of the crude reaction medium revealed the presence of both 1,4-dihydroquinolines **1d,e** and

quinolinium salts **2d,e**, which turned out to be extremely difficult to separate. Given this result, we decided to explore another route to obtain exclusively 1,4-dihydroquinoline **1d**. To overcome the alkylation reaction leading to undesirable compound **2e**, quinoline **4e** was first quaternized with methyl triflate to give the key intermediate **10** in 96% yield (Scheme 3). The resulting NHS-activated quinolinium **10**<sup>24</sup> was

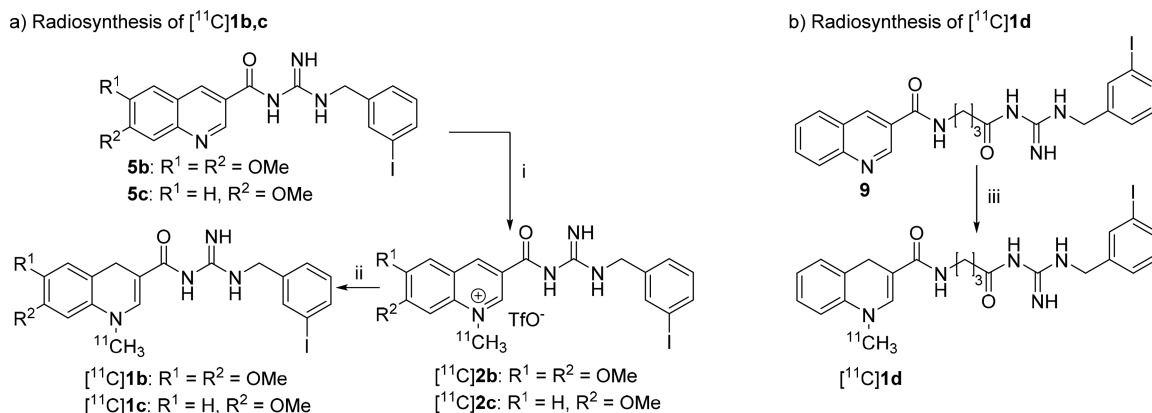
Scheme 3. Alternative Route to the Redox CDS-MIBG 1d<sup>a</sup>

<sup>a</sup>Reagents and conditions: (i)  $CH_3OTf$ ,  $CH_2Cl_2$ , 20 °C, 4 h (96%); (ii) polymer-bound DBU, **8b'**, THF, 20 °C, 12 h (58%); (iii) BNAH,  $CH_2Cl_2$ , 20 °C, 4 h (77% determined by  $^1H$  NMR).

smoothly reacted with linker-MIBG derivative **8b'** to yield compound **2d** (58%). Finally, a classical reduction reaction with BNAH led to the desired MIBG-targeting system **1d** (77% determined by  $^1H$  NMR).

Radiosyntheses of [ $^{11}C$ ]**1b,c** were carried out as depicted in Scheme 4 according to a two-step synthetic procedure.<sup>15,16,25</sup> The structures of the  $^{11}C$ -labeled products were confirmed by comparing their retention time with the corresponding nonradioactive standard compounds using reverse-phase HPLC. Thus, the quaternization reaction of quinolines **5b,c** with [ $^{11}C$ ]methyl triflate afforded quinolinium salts [ $^{11}C$ ]**2b,c**. Reduction of [ $^{11}C$ ]**2b,c** was conducted with BNAH for 5 min at 100 °C to provide the corresponding 1,4-dihydroquinolines [ $^{11}C$ ]**1b,c** (respectively, 68% and 61% relative percentages determined by radio-HPLC). The same procedure was applied to the radiosynthesis of [ $^{11}C$ ]**1d**. However, radio-HPLC analyses demonstrated that [ $^{11}C$ ]**2d** was not stable enough under these high dilution reaction conditions. To circumvent the poor stability of [ $^{11}C$ ]**2d**, we decided to add the reducing agent BNAH and the alkylating agent [ $^{11}C$ ] $CH_3OTf$  simultaneously. Then, the reaction mixture was left to react 5 min at 20 °C. To prevent [ $^{11}C$ ]**1d** from oxidation during the purification step, basic HPLC conditions were required. So, by adding triethylamine in HPLC eluent, 1,4-dihydroquinoline [ $^{11}C$ ]**1d** was obtained with a radiochemical purity of 50% (based on HPLC analysis of the crude product). A TRACERlab FX-MeI and FX-M radiosynthesis module was used to achieve a fully automated radiosynthesis of [ $^{11}C$ ]**1b-d** using a two-step reaction as shown in Scheme 4. The total synthesis time of the fully automated process was approximately 50 min. Activity levels in the final product ranged from 592 to 814 MBq for [ $^{11}C$ ]**1b**; 259–444 MBq for [ $^{11}C$ ]**1c**; and 148–518 MBq for [ $^{11}C$ ]**1d**. The radiochemical purities of [ $^{11}C$ ]**1b-d** were >95%.

Then, biological studies were conducted in rats to determine, *in vivo*, the cerebral penetration through the BBB of the different MIBG-targeting systems [ $^{11}C$ ]**1b-d** by measuring the radioactivity of the cerebral samples obtained after sacrifice of the animals (Figure 2). Last but not least, we

Scheme 4. Radiosyntheses of  $[^{11}\text{C}]1\text{b-d}^a$ 

<sup>a</sup>Reagents and conditions: for  $[^{11}\text{C}]1\text{b,c}$  from **5b,c**: (i)  $[^{11}\text{C}]\text{CH}_3\text{OTf}$ ,  $\text{CH}_3\text{CN}$ ,  $20\text{ }^\circ\text{C}$ , 5 min; (ii) BNAH,  $\text{CH}_3\text{CN}$ ,  $100\text{ }^\circ\text{C}$ , 5 min; for  $[^{11}\text{C}]1\text{d}$  from **9**: (iii)  $[^{11}\text{C}]\text{CH}_3\text{OTf}$ ,  $\text{CH}_3\text{CN}$ ,  $20\text{ }^\circ\text{C}$  and BNAH, then 10 min,  $20\text{ }^\circ\text{C}$ .

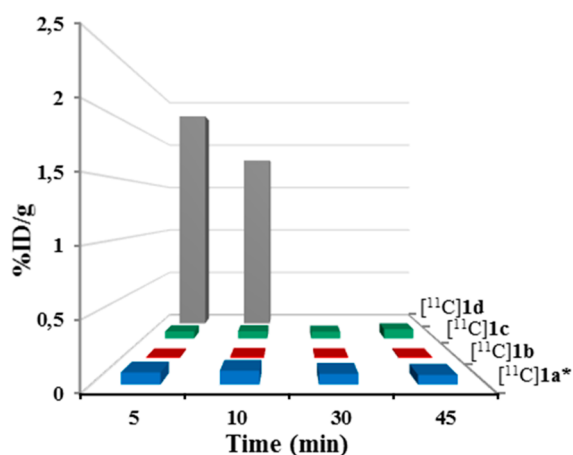


**Figure 2.** *Ex vivo* biodistribution of the radioactivity in rat brain at different time intervals following tail vein injection of  $[^{11}\text{C}]1\text{a-d}$  (5, 10, 30, and 45 min for  $[^{11}\text{C}]1\text{a-c}$ ; 5 and 10 min for  $[^{11}\text{C}]1\text{d}$ ). Results are expressed in percent of injected dose per gram (%ID/g, mean,  $n = 2$  for each point).  $[^{11}\text{C}]1\text{a}^*$  results are from ref 15.

quinolinium salts  $[^{11}\text{C}]2\text{b-d}$ , which subsequently led to the 200 cleavage of MIBG from the carrier through hydrolysis. The 201 results will be compared to those already obtained from  $[^{11}\text{C}]$  202 **1a**<sup>15</sup> in order to select the most promising CDS to target 203 MIBG to the CNS. 204

Then, the monitoring of both oxidation and MIBG cleavage 205 steps in the CNS were investigated from brain samples, which 206 were analyzed by radio-HPLC after radiotracer injection. Both 207 CDS-MIBG  $[^{11}\text{C}]1\text{b}$  and  $[^{11}\text{C}]1\text{c}$  proved to be rather stable 208 since 87% and 90% of 1,4-dihydroquinolines  $[^{11}\text{C}]1\text{b,c}$ , 209 respectively, were detected at 10 min after injection, together 210 with 12% and 5% of quinolinium salts  $[^{11}\text{C}]2\text{b,c}$ , respectively, 211 but with no traces of carboxylic acids  $[^{11}\text{C}]3\text{b,c}$  (Figure 3b,c). 212 <sup>15</sup> Regarding CDS-MIBG  $[^{11}\text{C}]1\text{a}$  previously investigated,<sup>15</sup> the 213 percentage of carboxylic acid  $[^{11}\text{C}]3\text{a}$  reached 11% at 10 min 214 after injection, highlighting a faster cleavage of MIBG from the 215 quinolinium salt **2a** (Figure 3a). We can therefore draw the 216 conclusion that the presence of methoxy groups on the carrier 217 do not increase the oxidation rates of  $[^{11}\text{C}]1\text{b,c}$  in the brain 218 compared to  $[^{11}\text{C}]1\text{a}$  and even seems to delay the cleavage of 219 MIBG from the resulting quinolinium salts  $[^{11}\text{C}]2\text{b,c}$ . 220

At this stage, it seems that in terms of brain uptake, 221 oxidation, and hydrolysis rates, CDS-MIBG  $[^{11}\text{C}]1\text{a}$  remains 222 the best candidate among the three CDS-MIBG  $[^{11}\text{C}]1\text{a-c}$ . In 223

198 were also interested (both in brain and plasma) in the 199 oxidation rates of  $[^{11}\text{C}]1\text{b-d}$  into the corresponding

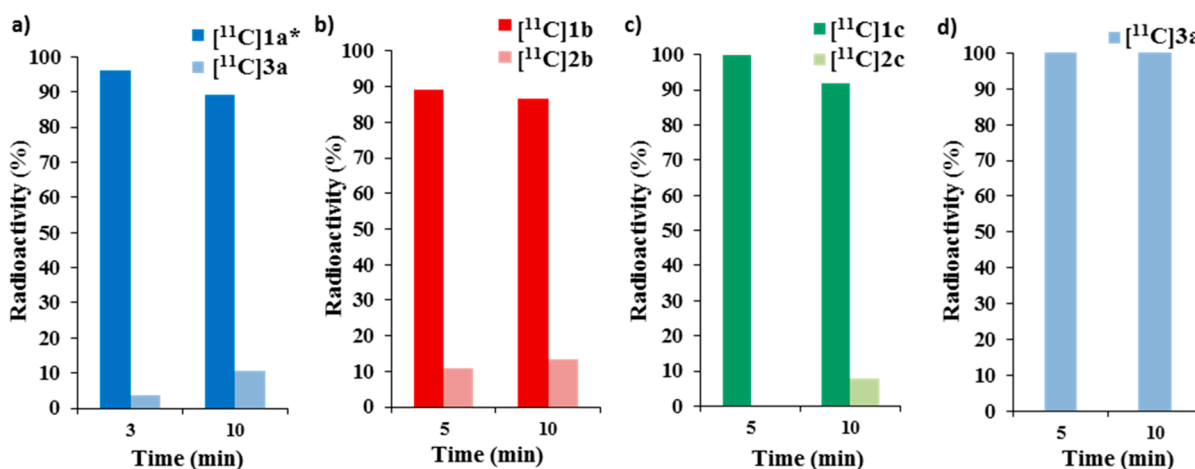
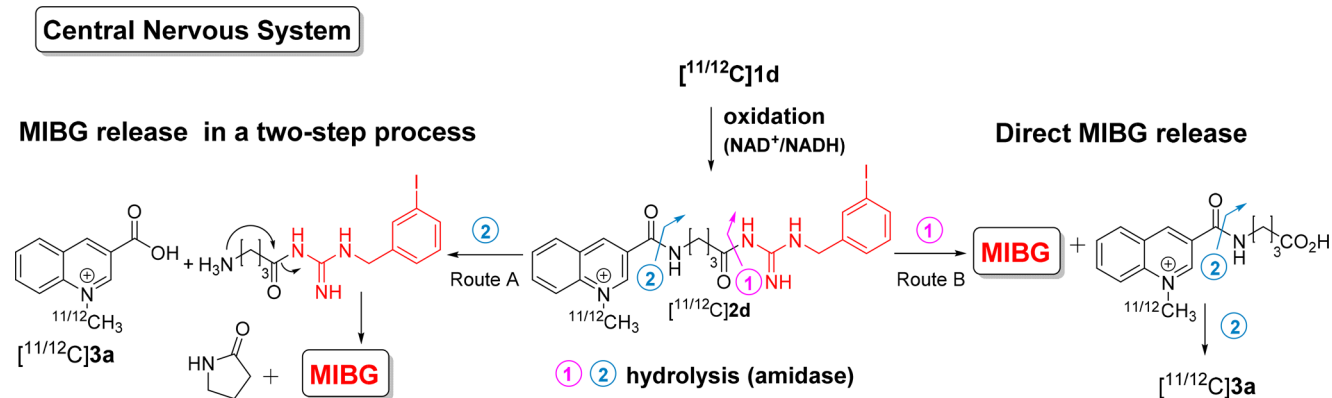


**Figure 3.** Percentage of the expected  $[^{11}\text{C}]$ radioactive species in brain after injection into rat of (a)  $[^{11}\text{C}]1\text{a}$ , (b)  $[^{11}\text{C}]1\text{b}$ , (c)  $[^{11}\text{C}]1\text{c}$ , and (d)  $[^{11}\text{C}]1\text{d}$  (mean,  $n = 2$  for each time point).  $[^{11}\text{C}]1\text{a}^*$  results are from ref 15.

Scheme 5. Schematic Representation for MIBG Release from Carrier-linker-MIBG 1d



224 contrast, HPLC analyses of both brain and plasma samples at 5  
 225 min after injection of 1,4-dihydroquinoline [ $^{11}\text{C}$ ]1d revealed  
 226 the presence of only one polar radioactive compound  
 227 corresponding to the carboxylic acid [ $^{11}\text{C}$ ]3a (Figure 3d).  
 228 These data indicate a fast *in vivo* oxidation of [ $^{11}\text{C}$ ]1d followed  
 229 by hydrolysis of the resulting quinolinium salt [ $^{11}\text{C}$ ]2d leading  
 230 to the release of carboxylic acid [ $^{11}\text{C}$ ]3a along with the linker-  
 231 MIBG intermediate, which would undergo cyclization to  
 232 produce desired MIBG along with  $\gamma$ -lactam as byproduct. This  
 233 scenario depicted in Scheme 5 (route A) is backed up by the  
 234 fact that during the preparation of 8b,b', a fast cyclization  
 235 process of the corresponding free amine was observed leading  
 236 to MIBG and  $\gamma$ -lactam products. At this stage, a second  
 237 scenario cannot be ruled out in which hydrolysis would occur  
 238 at the carbonyl group attached to MIBG as shown in Scheme 5  
 239 (route B) to release MIBG in a single step. In light of our  
 240 results, it might be concluded that the presence of a linker  
 241 between the 1,4-dihydroquinoline moiety and MIBG increases  
 242 notably not only the BBB passage and oxidation rate of [ $^{11}\text{C}$ ]  
 243 1d but also the release of MIBG from the carrier in the brain.  
 244 In this study, we successfully synthesized and labeled with  
 245 carbon-11 various [ $^{11}\text{C}$ ]CDS-MIBG ([ $^{11}\text{C}$ ]1b–d). We also  
 246 examined *in vivo* their potential to deliver MIBG into the  
 247 central nervous system. A preclinical evaluation showed high  
 248 BBB permeability of the carrier-linker-MIBG [ $^{11}\text{C}$ ]1d as  
 249 demonstrated by the high percentage of radioactivity measured  
 250 in the brain, whereas the two other CDS-MIBG [ $^{11}\text{C}$ ]1b,c  
 251 exhibited poor BBB passage. Once in the brain, fast oxidation  
 252 of the 1,4-dihydroquinoline [ $^{11}\text{C}$ ]1d and prompt cleavage of  
 253 MIBG from the resulting quinolinium salt [ $^{11}\text{C}$ ]2d take place  
 254 as evidenced by the only presence of carboxylic acid [ $^{11}\text{C}$ ]3a in  
 255 brain samples after 5 min. In light of these promising *in vivo*  
 256 profiles observed with [ $^{11}\text{C}$ ]1d, this work paves the way to the  
 257 use of the CDS-radiolabeled-MIBG as an appealing imaging  
 258 tool for the study of cerebral adrenergic nerve endings within  
 259 the brain.<sup>26272829</sup>

## 260 ■ ASSOCIATED CONTENT

### 261 ● Supporting Information

262 The Supporting Information is available free of charge on the  
 263 ACS Publications website at DOI: 10.1021/acsmchem-  
 264 lett.8b00642.

265 Experimental procedures and characterization of all  
 266 compounds, radiosyntheses and procedures for *in vivo*  
 267 experiments (PDF)

## ■ AUTHOR INFORMATION

### Corresponding Authors

\*E-mail: [gourand@cyceron.fr](mailto:gourand@cyceron.fr).

\*E-mail: [vincent.levacher@insa-rouen.fr](mailto:vincent.levacher@insa-rouen.fr).

### ORCID

Fabienne Gourand: 0000-0002-3585-6437

Vincent Levacher: 0000-0002-6429-1965

### Author Contributions

The manuscript was written through contributions of all authors. All authors have given approval to the final version of the manuscript;

### Notes

The authors declare no competing financial interest.

## ■ ACKNOWLEDGMENTS

This study was supported by a grant from CEA (Commissariat à l'Énergie Atomique et aux Énergies Alternatives), Labex IRON (ANR-11-LABX-0018-01), INSA-Rouen, Rouen University, CNRS, Labex SynOrg (ANR-11-LABX-0029), and Région Normandie. D.P. was supported by a grant "CIFRE" from Région Basse-Normandie and Cyclopharma laboratories. A.H. was supported by a grant from Région Haute-Normandie (Grant: CRUNCH 6-13).

## ■ ABBREVIATIONS

MIBG, *meta*-iodobenzylguanidine; NET, norepinephrine transporter; BBB, blood–brain barrier; CDS, chemical delivery system; SPECT, single photon emission computed tomography; PET, positron emission tomography; CNS, central nervous system; ADHD, attention deficit hyperactivity disorder

## ■ REFERENCES

- (1) Goldstein, D. S.; Eisenhofer, G.; Flynn, J. A.; Wand, G.; Pacak, K. Diagnosis and Localization of Pheochromocytoma. *Hypertension* 2004, 43, 907–910.
- (2) Cryer, P. E. Pheochromocytoma. *West. J. Med.* 1992, 156, 399–407.
- (3) Brisse, H.; Edeline, V.; Michon, J.; Couanet, D.; Zucker, J.; Neuenschwander, S. Current strategy for the imaging of neuroblastoma. *J. Radiol.* 2001, 82, 447–54.
- (4) Zhang, H.; Huang, R.; Pillarsetty, N.; Thorek, D. L.; Vaidyanathan, G.; Serganova, I.; Blasberg, R. G.; Lewis, J. S. Synthesis and evaluation of 18F-labeled benzylguanidine analogs for targeting the human norepinephrine transporter. *Eur. J. Nucl. Med. Mol. Imaging* 2014, 41, 322–332.

- (5) Zhang, H.; Huang, R.; Cheung, N.-K. V.; Guo, H.; Zanzonico, P. B.; Thaler, H. T.; Lewis, J. S.; Blasberg, R. G. Imaging the Norepinephrine Transporter in Neuroblastoma: A Comparison of [18F]-MFBG and 123I-MIBG. *Clin. Cancer Res.* **2014**, *20*, 2182–2191.
- (6) Hu, B.; Vavere, A. L.; Neumann, K. D.; Shulkin, B. L.; DiMugno, S. G.; Snyder, S. E. A Practical, Automated Synthesis of meta-[18F]Fluorobenzylguanidine for Clinical Use. *ACS Chem. Neurosci.* **2015**, *6*, 1870–1879.
- (7) Pandit-Taskar, N.; Zanzonico, P.; Staton, K. D.; Carrasquillo, J. A.; Reidy-Lagunes, D.; Lyashchenko, S.; Burnazi, E.; Zhang, H.; Lewis, J. S.; Blasberg, R.; Larson, S. M.; Weber, W. A.; Modak, S. Biodistribution and Dosimetry of 18F-Meta-Fluorobenzylguanidine: A First-in-Human PET/CT Imaging Study of Patients with Neuroendocrine Malignancies. *J. Nucl. Med.* **2018**, *59*, 147–153.
- (8) Baulieu, J. L.; Huguet, F.; Chalon, S.; Gerard, P.; Frangin, Y.; Besnard, J. C.; Pourcelot, L.; Guilloteaue, D. [<sup>125</sup>I]MIBG uptake and release in different regions of the rat brain. *Nucl. Med. Biol.* **1990**, *17*, 511–514.
- (9) Prokai, L.; Prokai-Tatrai, K.; Bodor, N. Targeting drugs to the brain by redox chemical delivery systems. *Med. Res. Rev.* **2000**, *20*, 367–416.
- (10) Bodor, N.; Buchwald, P. Barriers to remember: brain-targeting chemical delivery systems and Alzheimer's disease. *Drug Discovery Today* **2002**, *7*, 766–774.
- (11) Bodor, N.; Venkatraghavan, V.; Winwood, D.; Estes, K.; Brewster, M. E. Improved delivery through biological membranes. XLI. Brain-enhanced delivery of chlorambucil. *Int. J. Pharm.* **1989**, *53*, 195–208.
- (12) Wu, W. M.; Pop, E.; Shek, E.; Bodor, N. Brain-specific chemical delivery systems for beta-lactam antibiotics. In vitro and in vivo studies of some dihydropyridine and dihydroisoquinoline derivatives of benzylpenicillin in rats. *J. Med. Chem.* **1989**, *32*, 1782–1788.
- (13) Pop, E.; Bodor, N. Chemical systems for delivery of antiepileptic drugs to the central nervous system. *Epilepsy Res.* **1992**, *13*, 1–16.
- (14) Bodor, N.; Buchwald, P. *Soft Drugs in Retrometabolic Drug Design and Targeting*; John Wiley & Sons, Inc.: Hoboken, NJ, 2012.
- (15) Gourand, F.; Mercey, G.; Ibazizène, M.; Tirel, O.; Henry, J.; Levacher, V.; Perrio, C.; Barré, L. Chemical delivery system of Metaiodobenzylguanidine (MIBG) to the central nervous system. *J. Med. Chem.* **2010**, *53*, 1281–1287.
- (16) Gourand, F.; Tîntaş, M.-L.; Henry, A.; Ibazizène, M.; Dhilly, M.; Fillesoye, F.; Papamicaël, C.; Levacher, V.; Barré, L. Delivering FLT to the Central Nervous System by Means of a Promising Targeting System: Synthesis, [<sup>11</sup>C]Radiosynthesis and *in Vivo* Evaluation. *ACS Chem. Neurosci.* **2017**, *8*, 2457–2467.
- (17) Tedjamulia, M. L.; Srivastava, P. C.; Knapp, F. F., Jr. Evaluation of the brain-specific delivery of radioiodinated (iodophenyl) alkyl-substituted amines coupled to a dihydropyridine carrier. *J. Med. Chem.* **1985**, *28*, 1574–1580.
- (18) Benoit, R.; Dupas, G.; Bourguignon, J.; Quéguiner, G. Facile synthesis of annelated NADH model precursors. *Synthesis* **1987**, *12*, 1124–1126.
- (19) Charpentier, P.; Lobregat, V.; Levacher, V.; Dupas, G.; Quéguiner, G.; Bourguignon, J. An efficient synthesis of 3-cyanoquinoline derivatives. *Tetrahedron Lett.* **1998**, *39*, 4013–4016.
- (20) Woodman, D. J.; Davidson, A. I. N-Acylation during the addition of carboxylic acids to N-tert-butylacetylketenimines and the use of the reagent N-tert-butyl-5-methylisoxazolium perchlorate for peptide synthesis. *J. Org. Chem.* **1973**, *38*, 4288–4295.
- (21) Zhang, X.-B.; Waibel, M.; Hasserodt, J. An autoimmolative spacer allows first-time incorporation of a unique solid-state fluorophore into a detection probe for acyl hydrolases. *Chem. - Eur. J.* **2010**, *16*, 792–795.
- (22) DeWit, M. A.; Gillies, E. R. Design, synthesis, and cyclization of 4-aminobutyric acid derivatives: potential candidates as self-immolative spacers. *Org. Biomol. Chem.* **2011**, *9*, 1846–1854.
- (23) Alouane, A.; Labruère, R.; Le Saux, T.; Schmidt, F.; Jullien, L. Self-immolative spacers: kinetic aspects, structure-property relationships, and applications. *Angew. Chem., Int. Ed.* **2015**, *54*, 7492–7509.
- (24) Barré, A.; Tîntaş, M.-L.; Levacher, V.; Papamicaël, C.; Gembus, V. An overview of the synthesis of highly versatile N-hydroxysuccinimide esters. *Synthesis* **2017**, *49*, 472–483.
- (25) Bohn, P.; Gourand, F.; Papamicaël, C.; Ibazizène, M.; Dhilly, M.; Gembus, V.; Alix, F.; Tintas, M.-L.; Marsais, F.; Barré, L.; Levacher, V. Dihydroquinoline carbamate derivatives as bio-oxidizable >> prodrugs for brain delivery of acetylcholinesterase inhibitors: [<sup>11</sup>C] radiosynthesis and biological evaluation. *ACS Chem. Neurosci.* **2015**, *6*, 737–744.
- (26) Jewett, D. M. A simple synthesis of [<sup>11</sup>C]methyl triflate. *Int. J. Rad. Appl. Instrum. A* **1992**, *43*, 1383–1385.
- (27) Mauzerall, D.; Westheimer, F. H. 1-Benzylidihydronicotinamide - A model for reduced DPN. *J. Am. Chem. Soc.* **1955**, *77*, 2261–2264.
- (28) Wieland, D. M.; Wu, J.-L.; Brown, L. E.; Mangner, T. J.; Swanson, D. P.; Beierwaltes, W. H. Radiolabeled adrenergic neuron-blocking agents: adrenomedullary imaging with [<sup>131</sup>I]-Iodobenzylguanidine. *J. Nucl. Med.* **1980**, *21*, 349–353.
- (29) Wieland, D. M.; Mangner, T. J.; Inbasekaran, M. N.; Brown, L. E.; Wu, J.-L. Adrenal medulla imaging agents: a structure-distribution relationship study of radiolabeled aralkylguanidines. *J. Med. Chem.* **1984**, *27*, 149–155.